



Study of the corrosion behavior of magnesium alloy weldings in NaCl solutions by gravimetric tests

José A. Segarra[✉], Borja Calderón, Antonio Portolés

Universidad Politécnica de Madrid (UPM), E.T.S. de Ingenieros Industriales, Departamento de Física Aplicada e Ingeniería de Materiales, Calle de José Gutiérrez Abascal 2, 28006 Madrid

[✉]Corresponding author: jsegarra79@gmail.com

Submitted: 18 May 2015; Accepted: 7 September 2015; Available On-line: 14 October 2015

ABSTRACT: In this article, the corrosion behavior of commercial AZ31 welded plates in aqueous chloride media was investigated by means of gravimetric techniques and Neutral Salt Spray tests (NSS). The AZ31 samples tested were welded using Gas Tungsten Arc Welding (GTAW) and different filler materials. Material microstructures were investigated by optical microscopy to establish the influence of those microstructures in the corrosion behavior. Gravimetric and NSS tests indicate that the use of more noble filler alloys for the sample welding, preventing the reduction of aluminum content in weld beads, does not imply a better corrosion behavior.

KEYWORDS: AZ31; Corrosion; Immersion test; GTAW; NSS test

Citation / Cómo citar este artículo: Segarra, J.A., Calderón, B., Portolés, A. (2015) "Study of the corrosion behavior of magnesium alloy weldings in NaCl solutions by gravimetric tests". *Rev. Metal.* 51(3): e050. doi: <http://dx.doi.org/10.3989/revmetalm.050>.

RESUMEN: *Estudio del comportamiento frente a la corrosión de soldaduras de aleación de magnesio mediante técnicas gravimétricas.* En este artículo se ha investigado el comportamiento frente a la corrosión en medios acuosos salinos de chapas soldadas de aleación AZ31 mediante técnicas gravimétricas y ensayo en cámara de niebla salina. Las muestras estudiadas han sido soldadas mediante soldadura TIG (Tungsten Inert Gas) y con diferentes materiales de aporte. En el estudio se ha empleado microscopía óptica para analizar la microestructura. Los ensayos de gravimetría y los ensayos de niebla salina indican que el empleo de materiales de aporte más nobles para soldar las muestras evitando la disminución del contenido en aluminio en los cordones, no implica un mejor comportamiento frente a la corrosión.

PALABRAS CLAVE: AZ31; Corrosión; Ensayos cámara niebla salina; Ensayos gravimétricos; TIG

Copyright: © 2015 CSIC. This is an open-access article distributed under the terms of the Creative Commons Attribution-Non Commercial (by-nc) Spain 3.0 License.

1. INTRODUCTION

Magnesium and its alloys constitute from the point of view of light alloys a very interesting group of materials. Their lightness represents a major advantage in structural applications, but it is not the only one; the mechanical properties at high temperature-fatigue strength, dimensional stability, and alkaline resistance - in comparison with plastic materials (Avedesiam and

Baker, 1999) are properties with multiple applications, but their poor corrosion behavior makes their use difficult. This corrosion behavior may be affected by several factors such as impurities, environmental conditions, superficial conditions and design (Korb, 1992).

Magnesium is a very electronegative material which can suffer different corrosion processes such as galvanic corrosion, pitting corrosion, filiform

corrosion, stress corrosion cracking, fatigue corrosion and according to some investigators, also intergranular corrosion (Zeng *et al.*, 2006).

In aqueous environments, the anodic and the cathodic reactions commonly accepted (Pardo *et al.*, 2008) takes place according to the reactions:



In this article, the corrosion behavior of magnesium alloys type AZ31 samples welded by means of Gas Tungsten Arc Welding (GTAW) in salt aqueous solutions is investigated, trying to clarify from an experimental point of view its corrosion resistance and to find numeric relations between the welding parameters and the corrosion rates for the different samples.

The AZ31 alloy is a wrought alloy 3% of aluminum, 1% zinc which is considered to have a good relative weldability (Avedesiam and Baker, 1999) but there are recommendations about how to perform this procedure, arc welding methods are preferred instead of the oxyacetylene one. Magnesium and its alloys are very reactive materials in presence of oxygen and they require special measurements to protect the molten metal and to prevent their ignition and self-combustion.

Magnesium and its alloys can be joined by stud welding, spot welding and other resistance-welding processes as well as electron-beam, friction, explosion, and ultrasonic. Recently there have been several papers investigating the use of laser (Zemin *et al.*, 2011; Srinivasan *et al.*, 2011) as welding method, revealing unexpected results from a corrosion point of view and pointing out how important is the microstructure of the welding in the mechanical behavior of this alloys.

However arc welding-inert gas methods are the most commonly used (Avedesiam and Baker, 1999); these methods, both GTAW and GMAW (Gas Metal Arc Welding), have the advantage of using inert gas to protect the molten metal. Argon and mixtures of argon and helium can be used for these welding processes; the use of pure helium is not recommended because it raises the current required and increases weld spatter. Voltage and current type are also important parameters to take into account in the welding of magnesium alloys, the formation of protective corrosion products in the surface of the samples complicates arc stability and the fusion of the metal, for this reason in arc welding methods is always recommended using direct current reverse polarity (also known as Direct Current Electrode Positive, DCEP) or alternate current to provide cathodic cleaning during the welding process.

For all those reasons GTAW using high purity argon was chosen as welding method. GTAW is a welding system which allows to obtain high quality weld joints while minimizing spots, arc instability, porosity and the lack of penetration that may happen in the case of other arc welding techniques such as Shielded Metal Arc Welding (SMAW) or laser (Ben-Hamu *et al.*, 2007).

Some studies suggest that the corrosion of magnesium alloys in aqueous media may be explained considering three different factors: the chemical composition of matrix phase α , the composition of the other phases present in the alloy and how those phases are distributed in the matrix (Ming-Chun *et al.*, 2009); all those factors can be modified during the welding process, modifying the distribution of the precipitates. About this point there is controversy about AZ31 phase identification. Although most of authors think that the influence of precipitated particles in the corrosion behavior is important, there is no agreement about their origins and compositions, especially in the case of phase β - $\text{Mg}_{17}\text{Al}_{12}$. Some publications indicate the presence of this phase at room temperature meanwhile other identified these particles as Mn-Al or Mn-Al-Zn compounds (Winzer *et al.*, 2009).

In relation to the previous factors involved in the corrosion behavior, there are several publications about these alloys in which it has been studied by means of gravimetric (Walton *et al.*, 2012; Feliu *et al.*, 2011) or electrochemical techniques the corrosion behavior of magnesium alloys considering different superficial treatments and manufacturing processes, as seen in the works of Zhang *et al.*, (2011), Lu *et al.*, (2012), or Snir *et al.*, (2012), the crystallographic structure (Xin *et al.*, 2011) or the grain size (Liao *et al.*, 2012), so that in this article it was decided to study the effect of thermal cycles produced by welding processes in corrosion resistance, in addition to the former ones.

For this purpose it was decided to use gravimetric techniques instead of electrochemical ones considering the difficulty to measure corrosion in a reliable way indicated by other authors (Shi *et al.*, 2010), and trying to complement other studies in which non-welded alloys have been studied by electrochemical technics (Ben-Hamu *et al.*, 2009).

The structure of the samples has been studied using optical microscopy, trying to identify the different phases involved in the welding of the AZ31 alloy, as mentioned before this is not an easy task especially if the difficulties found out by other authors are considered.

The object of this study is to define the corrosion behavior of welded joints, to determine by means of metallographic techniques the structures and the grain size of the different welding areas and to quantify the corrosion rates of the samples considering the filler metals used.

2. EXPERIMENTAL PROCEDURES

2.1. Materials

In this study different AZ31B alloy welded samples with different filler metals were used. The welded samples were plates of 200×150×3.2 mm, for the welding of the samples Gas Tungsten Arc Welding (GTAW) system with alternate current was chosen. Samples were welded using one pass in the front and one in the back, using two current levels, 120 A for the front pass and 80 A for the back pass. The voltage was around 17 V and the speed for each pass was around $3 \times 10^{-3} \text{ m s}^{-1}$.

As filler metals AZ31 and AZ92, 4 mm diameter rods were used, according to Avedesiam and Baker (1999), in the case of welding Mg-Al alloys it is recommended using as filler metals alloys with a higher content of aluminum to reduce the hot crack sensitivity of the weldings. Although this recommendation is logical from a metallurgical point of view, aluminum improves the mechanical strength and hardness of magnesium alloys and it makes wider the freezing range of the molten material, the effect of this dissimilar chemical composition in the corrosion behavior has not been studied recently, so that it was decided to include as filler metals the same alloy of the magnesium plates and the most dissimilar alloy recommended in the previous reference.

To carry out the tests, 50×12×3.2 mm samples with $1.6 \times 10^{-3} \text{ m}^2$ area surface were taken, according to the sample size used by other authors (Pardo *et al.*, 2008), in order to get comparative reference results.

In this research AZ31 alloy base metal samples get from non-welded plates and transversal samples of the welded joints, including the melted joint, heat-affected zone and base metal, were used.

The electrolyte used during testing was an aqueous solution of NaCl with the concentrations indicated in next chapter.

2.2. Corrosion tests

In this study two different gravimetric techniques were used. The first was an standard Neutral Salt Spray (NSS) tests according to international standard ISO 9227 (AENOR 2007); the electrolyte used was a 5% weight NaCl (PA-ACS-ISO) in order to reduce the influence of impurities in the corrosion processes. Immersion tests were also used, in this case immersing test samples directly in the 3.5% NaCl electrolyte.

2.2.1. Immersion test

The immersion test were carried out by immersing in 0.75 liters of NaCl 3.5% weight solution the samples, the mass of each sample was measured with a precision micrometric scale before testing.

For the analysis of the different factors and parameters which could influence in the corrosion behavior, corrosion tests were done using groups of three samples in order to discriminate the significant effects. The next parameters were considered as basis of the tests:

- Filler metal (AZ31/AZ92)
- Agitation of the electrolyte
- Relative surface of the welding beads and the base metal of the samples.

The tests were carried out in two groups with different test durations, the first one up to 496 hours, the second one up to 1200 hours (50 days). For the first testing group, the effect of the electrolyte movement on the corrosion rate was studied.

2.2.2. Neutral Salt Spray tests

In the case of the salt spray test, the chamber and the procedures described for Neutral Salt Spray tests in the international standard ISO 9227 (AENOR 2007) were followed. The salt spray chamber used has a volume of 0.4 m³ with a 125 liters capacity. The solution used was 50 g L⁻¹ NaCl, which gives a concentration about 5% in weight.

In these tests 12 samples similar to the used in the previous gravimetric tests were used. The values of the collection rates were kept within the limits allowed by the ISO standard 9227(AENOR 2013) both for temperature and pH values.

The tests were carried out during 15 days, measuring the mass of the samples at their end.

All samples were weighted before and after the test. Because of the thick layer of corrosion products appeared during the test, in order to evaluate the corrosion rate and the mass loss during NSS tests it was necessary to immerse the samples in chromic acid H₂CrO₄ to dissolve it.

3. RESULTS

3.1. Micrography study

The samples were cut, polished and etched with acetic-picric (10⁻² L acetic acid; 4.2 g picric acid; 10⁻² L H₂O and 7×10⁻² L ethanol) during 30–40 seconds, then washed with ethanol and dried with a blast of hot air.

The granulometry and micrographic study shows that the structure of the material as fabricated (hot rolled) presents fine grain size G9 in accordance with ISO-643 (AENOR 2013). The observed structure is coherent with a hexagonal compact (HC) system metal, with equiaxial grains of rich Mg α -matrix were numerous twins can be seen, as shown in Fig. 1 (a and b) and Fig. 2 (a and b). The samples obtained directly from hot rolled sheets (as fabricated) and the

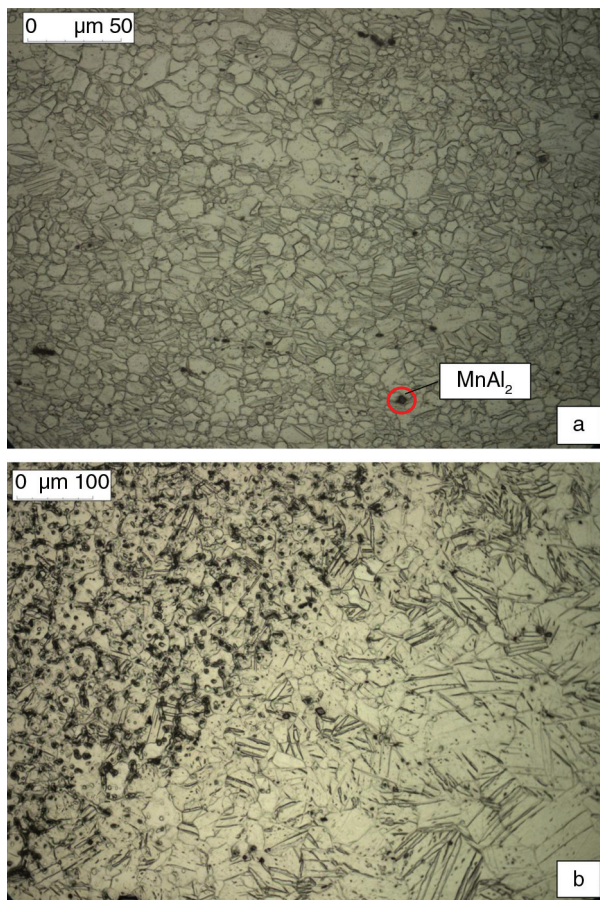


FIGURE 1. a) AZ31B plate micrography (X500); b) detail of a cross section welding joint, the heat-affected zone and the melted material (X200). Detail of $MnAl_2$ particles is included (identification according to Pardo *et al.*, 2008).

base metal of the welded specimens show small precipitated particles, according to Pardo *et al.*, (2008), being the dark grey dispersed grains $MnAl_2$, and according to Avedesiam and Baker (1999) the small precipitated particles being β -phase $Mg_{17}Al_{12}$.

Weld beads have a dendritic structure with a grain size slightly larger, between $G=7.5$ and $G=6$ units and as mentioned before, precipitate particles of β -phase $Mg_{17}Al_{12}$ or Mn-Al compounds are observed spread in the α -matrix phase (Fig. 3a). The amount of β phase/Mn-Al is clearly different in the AZ31 and the AZ92 filler metal welded samples, as well as the grain size, which is clearly coarser in the case of the samples welded with AZ31 than in the AZ92 ones. The amount of spread β -phase/Mn-Al particles is larger in the case of AZ92 welded samples. Precipitated particles are located all over the matrix of α -phase and no preferential precipitation zones were found out in this study.

In the case of the Heat-Affected Zone (HAZ) its grain size varies between $G=7$ and $G=3$, grain size is larger in the HAZ of welded samples using AZ92 as filler metal (Fig. 3a). The presence of precipitated

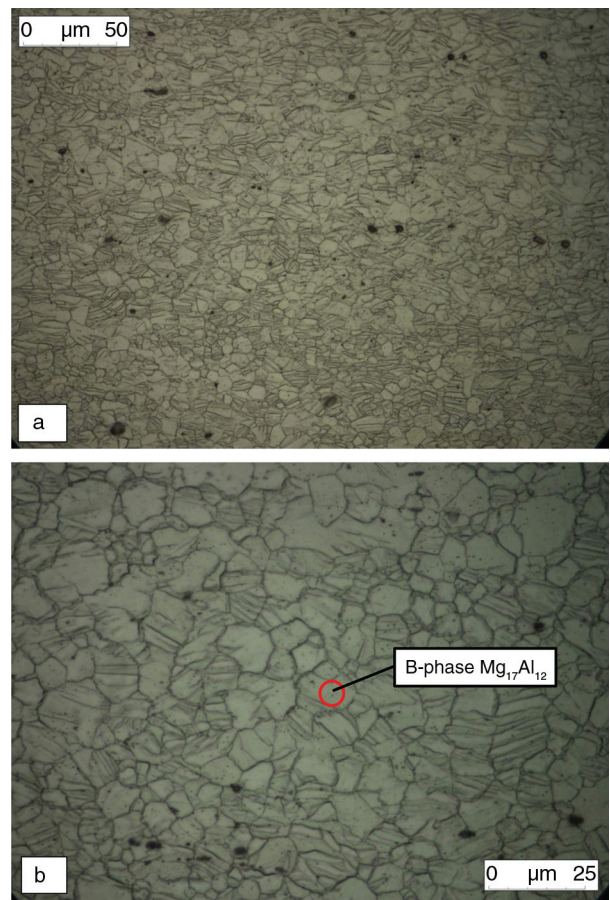


FIGURE 2. a) Base metal (X200); b) base metal detail. Twins can be seen inside the crystals. (X1000). β -phase precipitated particles are indicated (according to Avedesiam and Baker, 1999).

particles of β -phase/Mn-Al is less important in this area than for the region of melted material or the base metal.

Figure 4b summarizes grain sizes of the different samples and welding areas.

The study of corroded surfaces shows that the attack takes place in a section close to the HAZ, it starts as localized corrosion in the areas of larger grain size (corrosion resistance of AZ31B alloy tends to increase as grain size is reduced), probably due to the enhanced passivity of surface oxide films (Liao *et al.*, 2012). In the case of the neutral salt spray test it was not possible to establish a preferential mechanism due to the high grade of corrosion that specimens suffered.

3.2. Immersion tests

As previously stated, two different test rounds were done, the first one up to 406 hours, and the second one up to 1200 hours (50 days).

Immersion tests indicate the influence of the electrolyte agitation in corrosion rates. Values for

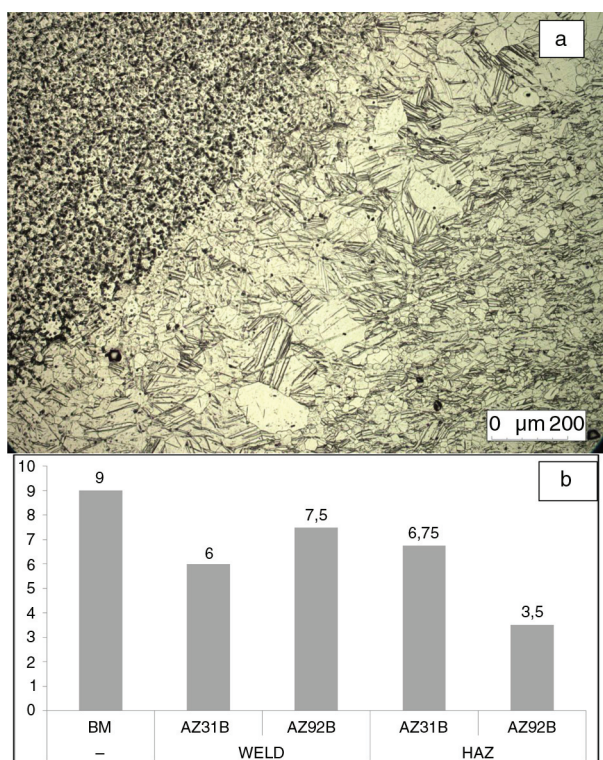


FIGURE 3. a) Detail of the HAZ compared with welded metal, upper-left corner, and base metal, down-right corner of the image (X100); b) grain size G of the samples according to the ISO-643 standard. Filler material is indicated for welded samples.

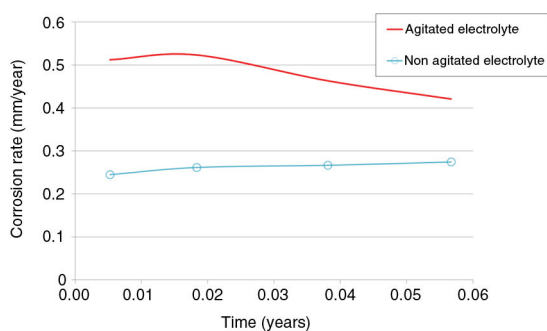


FIGURE 4. Comparative of the corrosion rate for electrolyte within and without agitation.

samples in electrolyte with agitation are between 0.35 and 0.51 mm/year meanwhile in tests carried out without agitation those values vary between 0.22 and 0.3 mm/year as indicated in graphic shown in Fig. 4.

Figure 5 shows mass loss per surface unit as a function of the immersion time; this graphic shows that a grade 2 polynomial law can be considered to represent the corrosion rate. In Table 1 the kinetic laws of the corrosion rate of the different samples are shown, and it can be observed that the relative movement of the electrolyte used has a significant influence in the corrosion rate.

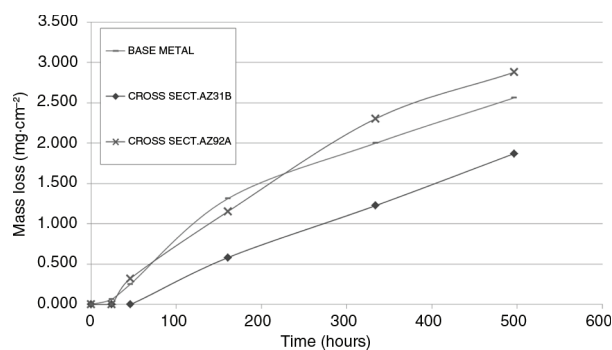


FIGURE 5. Mass loss per surface unit as function of time (hours). First round test.

During the second test round, the behavior of the samples was coherent with the previous results; again parabolic mathematical laws were obtained. Figure 6 shows mass loss as a function of time, and the obtained kinetics laws are indicated in Table 1.

3.3. Neutral Salt Spray tests

NSS test were carried out during 16 days. Figure 7 shows the mass loss observed at the end of the NSS test. The samples were heavily attacked during these tests; thick corrosion layers were produced all over the specimens so that no particular corrosion mechanism could be identified, but only a uniform corrosion aspect.

4. DISCUSSION

The resultant micrographies indicate that the cross sections of the sample plates show an equiaxed structure (see Fig. 1a and b) and the presence of small precipitated particles is clearly visible. As mentioned in the previous chapter, according to other authors (Ben-Hamu *et al.*, 2007) β -phase is not stable at room temperature, the presence of $Mg_{17}Al_{12}$ precipitated particles may be explained as follows: in the case of “as fabricated” material is very likely that β -phase precipitated particles are metastable compounds produced during the cooling of the hot rolling process, the same result could explain its presence in the melted material. The fast cooling rates during welding processes would help to produce metastable structures, this hypothesis is also supported by the small amount of dispersed particles present in the heat-affected zone. It can be argued that β -phase particles present in the as fabricated base material are dissolved during the thermal cycle of the welding, so that the presence of the β -phase metastable in the AZ31 alloy specimens has two explanations, the small dispersed particles present in the α -matrix are produced during the hot-rolling process and there are larger particles in the welded zones due to the freezing. The same explanation may

TABLE 1. Polynomic kinetic laws representing mass loss per surface unit (y, expressed at mg cm⁻²) as function of time (x, expressed at hours)

y	y=c·x ² +a·x+b			R ^{2*}	Name	SAMPLE DESCRIPTION		
	c [§] ×10 ⁻⁶	a [†] ×10 ⁻²	b [‡] ×10 ⁻²			Filler metal	Sample area	Description
First round tests (496 hours)								
x	-8	1.09	2.64	0.999	B1	–	Base metal	Agitated electrolyte
	-4	1.04	7.79	0.996	B2	–	Base metal	Agitated electrolyte
	-7	1.41	-15	0.998	B3	–	Base metal	Agitated electrolyte
	1	0.37	11.62	0.992	B4	–	Base metal	Agitated electrolyte
	0.8	5.80	6.88	0.998	B5	–	Base metal	Agitated electrolyte
	1	0.54	3.87	0.998	B6	–	Base metal	Agitated electrolyte
	-8	0.90	7.53	0.992	B7	–	Base metal	Agitated electrolyte
	0.2	0.38	7.69	0.994	MT	AZ31B	Cross section sample	Agitated electrolyte
	-6	0.90	10	0.996	TT	AZ92A	Cross section sample	Agitated electrolyte
	-4	0.64	1.11	0.987	B8	–	Base metal	Agitated electrolyte
Second round tests (1200 hours)								
	-3	1.08	39.44	0.987	M3A	AZ31B	Cross section sample	Agitated electrolyte
	-7	1.87	1150.3	0.984	T3B	AZ92A	Cross section sample	Agitated electrolyte
	-1	2.75	122	0.99	MBB	–	Base metal	Agitated electrolyte

[§]quadratic value coefficient of the polynomic expression.

[†]lineal value coefficient of the polynomic expression.

[‡]constant value coefficient of the polynomic expression.

*Regression coefficient.

be valid in the case of the Mg-Mn-Al compounds, the different morphology and their presence in weld beads and base metal may be easily explained considering them also as metastable particles at room temperature.

In samples welding areas precipitated particles are observed all over the melted region. Those particles are spread along the α -matrix and in the grain boundaries without preferential precipitation areas. Grain size is slightly larger than the observed in the base metal, this fact is coherent in welding processes (Fig. 3a and b), and although the morphology of the particles is almost the same, the amount of β -phase/Mn-Al compounds present in AZ31 filler

metal samples is less than in the AZ92. The chemical composition and grain refine properties of zinc can explain this behavior, and although the studied samples do not show preferential precipitation areas, it can be argued that grain size is involved in the way those particles precipitate into the matrix. It is very likely that grain boundaries act as inhibitors of the β -phase/Mn-Al particles growth.

The growth of the grain in the HAZ shown in Fig. 3a can be explained because of the thermal cycle during welding process, obtaining greater grain size values in the interphase between melted material and the HAZ than in the interphase with base metal. Another important fact is the lack of Mg₁₇Al₁₂/Mn-Al particles. Micrographs show that the presence of β -phase/Mn-Al particles is rare in the HAZ, especially where close to the melted zone. The main reason to understand this modification of the microstructure is that the particles are dissolved in the α -matrix. The same microstructures are shown by Jäger *et al.* (2006), although the authors of this article did not indicate about the presence of precipitates, the microstructures of the “as fabricated” materials are the same that those obtained in this research, showing small spots spread inside the α -matrix which disappear after the annealing treatments. The same clean microstructures in the welding’s heat-affected zones are obtained in this research, so that the relationship between thermal cycles/cooling rates and the presence of β -phase/Mn-Al can be established.

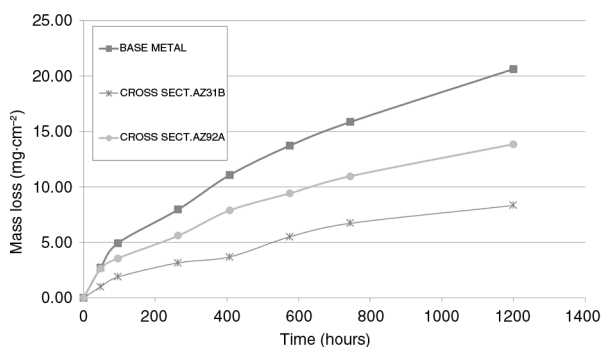


FIGURE 6. Mass loss per surface as function of time graphic. Second round test.

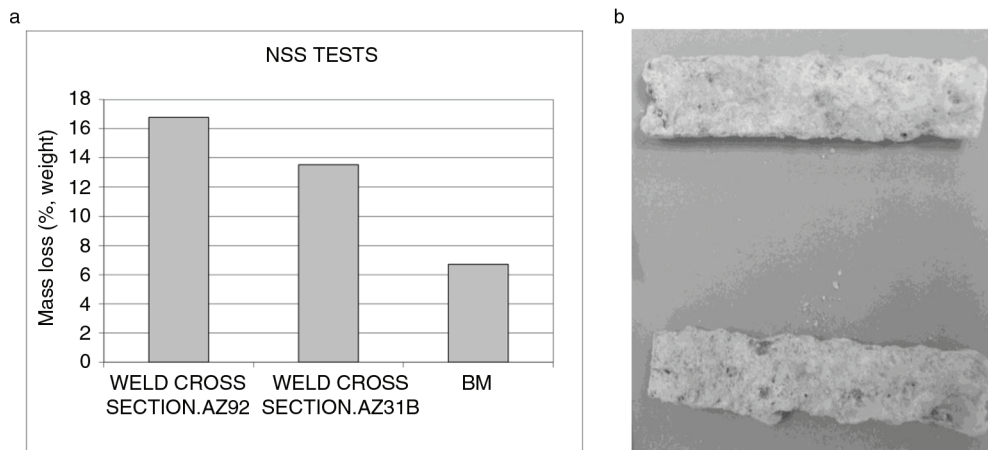


FIGURE 7. a) Mass loss in NSS test; b) samples after NSS test.

The obtained results in the NSS tests show that corrosion resistance is affected by welding processes, as can be seen in Fig. 7. The results indicate that, as in the case of the immersion tests, weldings using AZ92 as filler metal have worst behavior than the AZ31 filler metal weldings samples.

During immersion tests, welded samples shown corrosion rates lower than the obtained for base metal (see Fig. 5 and Fig. 6). This discrepancy between NSS and immersion tests could be explained by the different NaCl concentration and the exposure mechanism which produces porous layers of corrosion products with massive volume (Fig. 7b).

Immersion tests show parabolic laws to represent the corrosion rate as function of time. This behavior is probably related with the formation of protective corrosion layers, further investigation is needed about this hypothesis. For all tests the determination coefficients are close to 1, being better than in the case of linear approximations. However, as indicated in Table 1, it can be observed that values for quadratic components are very small and negative, between 10^{-5} and 10^{-7} , considering that in the case of linear correlations the determination coefficients are also close to 0.9 value, results indicate that corrosion rates could also be considered as lineal.

Corrosion rates of AZ31B filler metal welded samples are smaller than those obtained for AZ92 filler metal welded samples (Fig. 5 and Fig. 6). The statement that the higher content of aluminum in the filler metal, the less corrosion rate of the welding joint, has been already discussed and refused in other studies (Cheng *et al.*, 2009). Several hypothesis have been proposed to explain that fact, including that a higher proportion of aluminum does not imply a better corrosion resistance if the resulting structure generates anodic and cathodic areas or if the spread precipitates phases do not produce protective layers. As mentioned in the previous chapter, the corrosion process starts in the HAZ area, where the presence

of β /Mn-Al particles is rare. It means that from the corrosion point of view, there is no advantages of using a better chemical composition filler metal, as it seems that the thermal cycle produced by the welding dissolves the β -phase/Mn-Al particles and increases the grain the size in the HAZ in such a way that corrosion resistance cannot be improved by the chemical composition of the melted areas but just the opposite: the presence of a large cathodic area (the weld bead) close to the critic corrosion area of the HAZ may provide an additional electron supply to the anodic areas, so that, although from a mechanical and welding point of view there is no doubt about the advantages of increasing the amount of aluminum and zinc in filler metals, the use of a different chemical composition alloy can induce a non-expected electrochemical corrosion deterioration.

5. CONCLUSIONS

- Different welding processes do not imply a significant modification of AZ31B corrosion resistance in NaCl solutions if those welding's are done within right and qualified procedures.
- Obtained microstructures for welding processes must be taken into account as a major parameter in corrosion resistance.
- The use of noble filler materials (including higher content of aluminum) does not guarantee an improvement of welding joint corrosion resistance because anodic and cathodic zones can be formed reversing the improvement of a better chemical composition.

ACKNOWLEDGEMENTS

The authors would like to acknowledge the financial support by the Dpto. de Física Aplicada e Ingeniería de Materiales, E.T.S. Ingenieros Industriales de Madrid, Universidad Politécnica de Madrid.

REFERENCES

- AENOR (2013). Steel. Micrographic determination of the apparent grain size (ISO 643:2012). Ed. AENOR, Madrid.
- AENOR (2007). Corrosion tests in artificial atmospheres. Salt spray tests (ISO 9227:2006). Ed. AENOR, Madrid.
- Avedesian, M., Baker, H. (1999). *ASM Speciality Handbook. Magnesium alloys*, Ed. ASM International, Materials Park, Ohio (USA), pp. 3–4.
- Ben-Hamu, G., Eliezer, D., Cross, C.E., Böllinghaus, T. (2007). The relation between microstructure and corrosion behavior of GTA welded AZ31B magnesium sheet. *Mat. Sci. Eng. A* 452–453, 210–218. <http://dx.doi.org/10.1016/j.msea.2006.12.122>.
- Ben-Hamu, G., Eliezer, D., Wagner, L. (2009). The relation between severe plastic deformation microstructure and corrosion behavior of AZ31 magnesium alloy. *J. Alloy Compd.* 48 (1–2), 222–229. <http://dx.doi.org/10.1016/j.jallcom.2008.01.084>.
- Cheng, Y., Qin, T.-W., Wang, H.-M., Zhang, Z. (2009). Comparison of corrosion behaviors of AZ31, AZ91, AM60 and ZK60 magnesium alloys. *T. Nonferr. Metal. Soc. China* 19 (3), 517–524. [http://dx.doi.org/10.1016/S1003-6326\(08\)60305-2](http://dx.doi.org/10.1016/S1003-6326(08)60305-2).
- Feliu, S. Jr., Maffiotte, C., Galván, J.C., Barranco, V. (2011). Atmospheric corrosion of magnesium alloys AZ31 and AZ61 under continuous condensation conditions. *Corros. Sci.* 53 (3), 1865–1872. <http://dx.doi.org/10.1016/j.corsci.2011.02.003>.
- Jäger, A., Lukác, P., Gärtnerová, V., Haloda, J., Dopita, M. (2006). Influence of annealing on the microstructure of commercial Mg alloy AZ31 after mechanical forming. *Mat. Sci. Eng. A-Struct.* 432 (1–2), 20–25. <http://dx.doi.org/10.1016/j.msea.2006.06.070>.
- Korb, L.J. (1992). *ASM Handbook*, Vol. 13, Corrosion, ASM International, Materials Park, Ohio.
- Liao, J., Hotta, M., Yamamoto, N. (2012). Corrosion behavior of fine-grained AZ31B magnesium alloy. *Corros. Sci.* 61, 208–214. <http://dx.doi.org/10.1016/j.corsci.2012.04.039>.
- Lu, L., Liu, T., Chen, J., Wang, Z. (2012). Microstructure and corrosion behavior of AZ31 alloys prepared by dual directional extrusion. *Mater. Design.* 36, 687–693. <http://dx.doi.org/10.1016/j.matdes.2011.12.023>.
- Ming-Chun, Z., Schmutz, P., Brunner, S., Ming, L., Guang-Ling, S., Atrens, A. (2009). An exploratory study of the corrosion of Mg alloys during interrupted salt spray testing. *Corros. Sci.* 51 (6), 1277–1292. <http://dx.doi.org/10.1016/j.corsci.2009.03.014>.
- Pardo, A., Merino, M.C., Coy, A.E., Arrabal, R., Viejo, F., Matykina, E. (2008). Corrosion behaviour of magnesium/aluminium alloys in 3.5 wt.% NaCl. *Corros. Sci.* 50 (3), 823–834. <http://dx.doi.org/10.1016/j.corsci.2007.11.005>.
- Shi, Z., Liu, M., Atrens, A. (2010). Measurement of the corrosion rate of magnesium alloys using Tafel extrapolation. *Corros. Sci.* 52 (2), 579–588. <http://dx.doi.org/10.1016/j.corsci.2009.10.016>.
- Snir, Y., Ben-Hamu, G., Eliezer, D., Abramov, E. (2012). Effect of compression deformation on the microstructure and corrosion behavior of magnesium alloys. *J. Alloy Compd.* 528, 84–90. <http://dx.doi.org/10.1016/j.jallcom.2012.03.010>.
- Srinivasan, P.B., Riekehr, S., Blawert, C., Dietzel, W., Koçak, M. (2011). Mechanical properties and stress corrosion cracking behaviour of AZ31 magnesium alloy laser weldments. *T. Nonferr. Met. Soc. China* 21 (1), 1–8. [http://dx.doi.org/10.1016/S1003-6326\(11\)60670-5](http://dx.doi.org/10.1016/S1003-6326(11)60670-5).
- Walton, C.A., Martin, H.J., Horstemeyer, M.F., Wang, P.T. (2012). Quantification of corrosion mechanisms under immersion and salt-spray environments on an extruded AZ31 magnesium alloy. *Corros. Sci.* 56, 194–208. <http://dx.doi.org/10.1016/j.corsci.2011.12.008>.
- Winzer, N., Xu, P., Bender, S., Gross, T., Unger, W., Cross, C.E. (2009). Stress corrosion cracking of gas-tungsten arc welds in continuous-cast AZ31 Mg alloy sheet. *Corros. Sci.* 51 (9), 1950–1963. <http://dx.doi.org/10.1016/j.corsci.2009.05.037>.
- Xin, R., Li, B., Li, L., Liu, Q. (2011). Influence of texture on corrosion rate of AZ31 Mg alloy in 3.5 wt.% NaCl. *Mater. Design.* 32 (8–9), 4548–4552. <http://dx.doi.org/10.1016/j.matdes.2011.04.031>.
- Zemin, W., Ming, G., Haiguo, T., Xiaoyan, Z. (2011). Characterization of AZ31B wrought magnesium alloy joints welded by high power fiber laser. *Mater. Charact.* 62 (10), 943–951. <http://dx.doi.org/10.1016/j.matchar.2011.07.002>.
- Zeng, R., Zhang, J., Huang, W., Dietzel, W., Kainer, K.U., Blawert, C., Ke, W. (2006). Review of studies on corrosion of magnesium alloys. *T. Nonferr. Met. Soc. China* 16 (Sup. 2), s763–s771. [http://dx.doi.org/10.1016/S1003-6326\(06\)60297-5](http://dx.doi.org/10.1016/S1003-6326(06)60297-5).
- Zhang, T., Shao, Y., Meng, G., Cui, Z., Wang, F. (2011). Corrosion of hot extrusion AZ91 magnesium alloy: I-relation between the microstructure and corrosion behavior. *Corros. Sci.* 53 (5), 1960–1968. <http://dx.doi.org/10.1016/j.corsci.2011.02.015>.